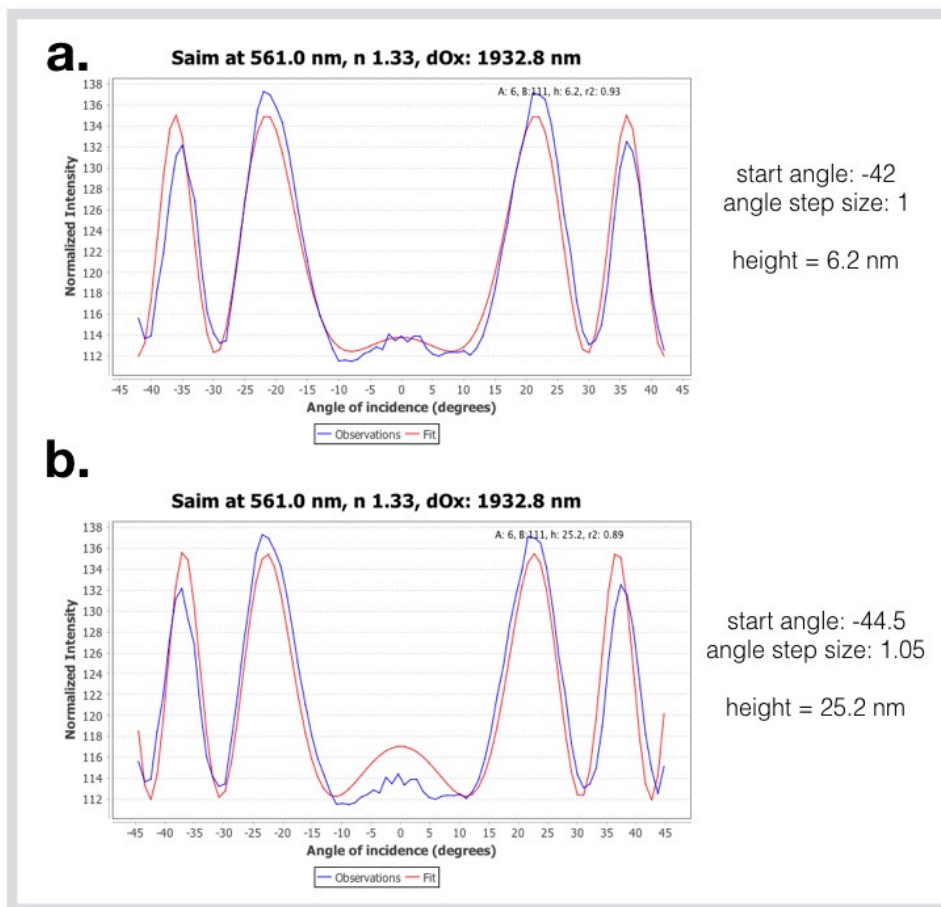


SUPPLEMENTARY INFORMATION:

A data acquisition and analysis pipeline for scanning angle interference microscopy

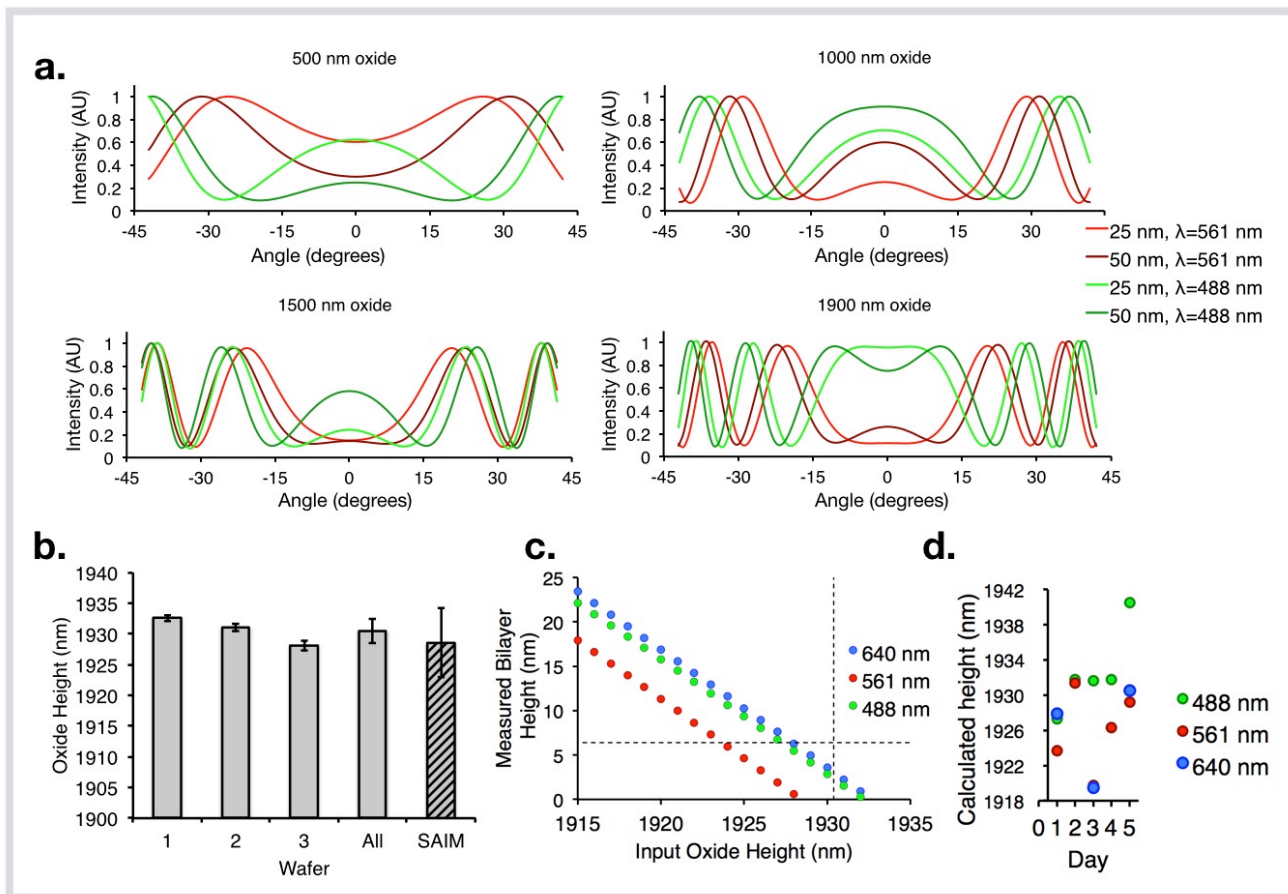
Catherine B. Carbone, Ronald D. Vale, and Nico Stuurman

Supplementary Figure 1.



Supplementary Figure 1. Error introduced by improper calibration. **(a)** Correctly calibrated data. SAIM Data from a DiI labeled supported lipid bilayer fit correctly. Intensity measurements were taken at 1-degree intervals from -42° to 42° . **(b)** Incorrectly calibrated data. The same data as in **a**, fit with a false calibration wherein the measurements were aligned to a start angle of -44.5° and an angle step size of 1.05° .

Supplementary Figure 2.



Supplementary Figure 2. Importance of precise measurement of oxide height. **(a)** Periodicity of SAIM function at differing oxide heights. Theoretical intensity is plotted vs. angle for 488 nm (green lines) or 561 nm (red lines) laser illumination at 25 (light lines) nm or 50 nm (dark lines) from the surface of the oxide. Four oxide heights are represented: 500 nm, 1000 nm, 1500 nm and 1900 nm. **(b)** Measurement of oxide layer thickness. Three separate wafers were measured by ellipsometry at 8 positions spaced at increments of ~ 1 cm apart. Error bars represent standard deviation of these eight measurements. “All” depicts the mean and standard deviation of 24 measurements across three wafers (1930.5 ± 2.0 nm). “SAIM” depicts the mean and standard deviation for the deduced oxide height at three wavelengths (488 nm, 561 nm, 647 nm), on two different microscopes and on five separate days (1928.5 ± 5.6 nm) for wafer #3. **(c)** Using SAIM to deduce oxide thickness. A triple labeled bilayer (DiO, DiI, DiD) was measured by SAIM at three wavelengths (488 nm, 561 nm, 647 nm). These data were then fit using oxide thicknesses ranging from 1915 nm to 1935 nm, which is plotted here versus the resultant sample height. Vertical dashed line represents the oxide thickness measured by ellipsometry (1930.5 ± 2.0 nm). Horizontal dashed line represents the expected height of the supported lipid bilayer (6.4 nm) [15]. Deduced oxide height is the intersection of the horizontal line for true bilayer height and the data. **(d)** Daily wavelength-dependent variation in oxide height measurements. Data for “SAIM” in **b** are shown as individual data points to highlight day-to-day variability.

Supplementary Note.

Formulas used for the analysis plugin are drawn from reference [8]. This reference contained a typographical error in the r^{TE} formula (3), which has been corrected here.

For incident light polarized perpendicular to the plane of incidence, the detected intensity variation at a given pixel in the image relates to the average height of the fluorophore and the angle of incidence as follows:

$$I = A(|1 + r^{TE} e^{i\phi(H)}|)^2 + B \quad (1)$$

where

A - accounts for variation in detected intensity due to factors including mean excitation laser intensity, fluorophore density, efficiency of emitted photon detection, etc..

B - is an offset parameter that accounts for background fluorescence in the sample images.

H - is the position above the silicon oxide layer

$\phi(H)$ - the phase difference of the direct and reflected light at axial position H given by:

$$\phi(H) = \frac{4\pi}{\lambda} (n_b H \cos\theta_b) \quad (2)$$

r^{TE} - the effective Fresnel coefficient obtained from the transfer matrix m^{TE} according to:

$$r^{TE} = \frac{(m_{11}^{TE} + m_{12}^{TE} p_0) p_2 + (m_{21}^{TE} - m_{22}^{TE} p_0)}{(m_{11}^{TE} + m_{12}^{TE} p_0) p_2 + (m_{21}^{TE} + m_{22}^{TE} p_0)} \quad (3)$$

where

$$m_{11}^{TE} = \cos(k_{ox} d_{ox} \cos\theta_{ox}) \quad (4)$$

$$m_{12}^{TE} = \frac{-i}{p_1} \sin(k_{ox} d_{ox} \cos\theta_{ox}) \quad (5)$$

$$m_{21}^{TE} = -ip_1 \sin(k_{ox} d_{ox} \cos\theta_{ox}) \quad (6)$$

$$m_{22}^{TE} = \cos(k_{ox} d_{ox} \cos\theta_{ox}) \quad (7)$$

$$p_0 = n_{Si} \cos\theta_{Si}, p_1 = n_{ox} \cos\theta_{ox}, p_2 = n_b \cos\theta_b \quad (8)$$

$$k_i = \frac{2\pi n_i}{\lambda} \quad (9)$$

k_i - wavenumber in the given material

n_{Si} - refractive index of silicon

n_{ox} - refractive index of the oxide layer

n_b - refractive index of the sample

θ_{Si} - angle of incidence in the silicon

θ_{ox} - angle of incidence in the oxide layer

θ_b - angle of incidence in the sample

By rewriting the effective Fresnel coefficient as a complex number:

$$r^{TE} = c + id \quad (10)$$

Equation 1 can then be rewritten as:

$$I = A(1 + 2ccos\phi(H) - 2dsin\phi(H) + c^2 + d^2) + B \quad (11)$$

Not only can equation 11 be computed about 10 times faster than equation 1, it can also be used to derive partial derivatives needed for Levenberg-Marquard non-linear least square curve fitting, using

$$f = \frac{d}{dH} \phi(H) = \frac{4\pi n_b \cos\theta_b}{\lambda} \quad (12)$$

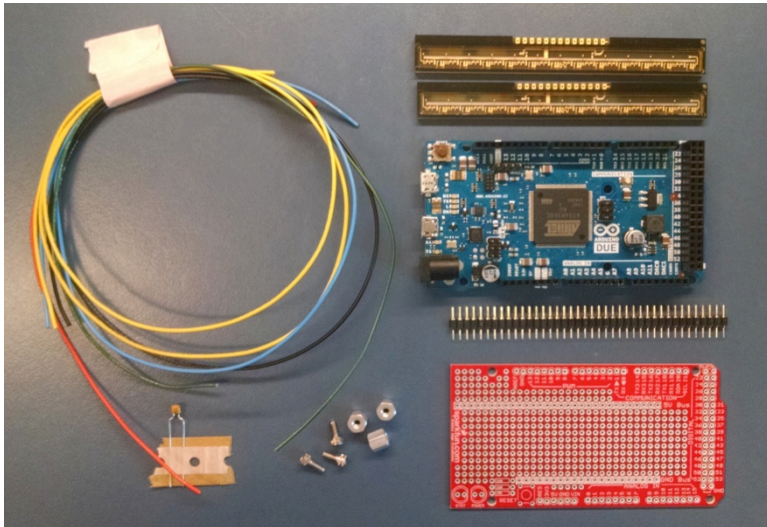
Partial derivative of equation 11 for H:

$$\frac{d}{dH} (I) = -2Af(csin\phi(H) + dcos\phi(H)) \quad (13)$$

Supplementary Protocol.

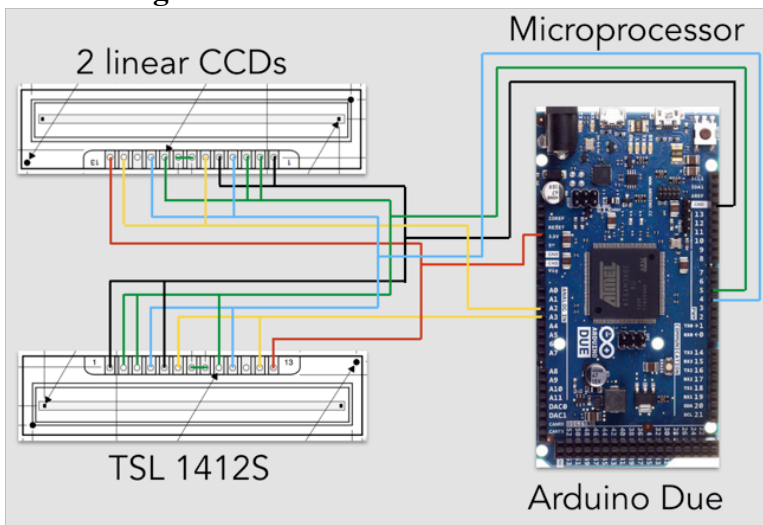
Building plans for laser angle calibration device. We designed a simple apparatus that consists of a clear, brightly colored acrylic front plate, and two linear CCDs detecting fluorescence emerging from the front plate. Using an automated procedure, this device defines the relation between motor position and angle within minutes and at much higher precision than possible using manual procedures. The building plans for this device and firmware are detailed here. Note that the precise pin used at each step is flexible as long as the physical arrangement of the detector matches the firmware code.

Parts needed:



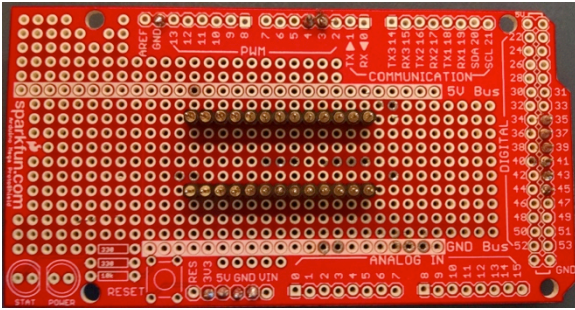
- 1 Arduino Due
- 2 TAOS Linear Sensor Array (TSL 1412S)
- 1 SparkFun MegaShield Kit (DEV-09346)
- 1 0.1 μF capacitor
- 3 0.25" hexagonal standoffs with screws
- SparkFun Break Away Headers - Machine Pin (PRT-00117)
- 24-gauge solid core wire

Circuit diagram for detectors connected in serial:



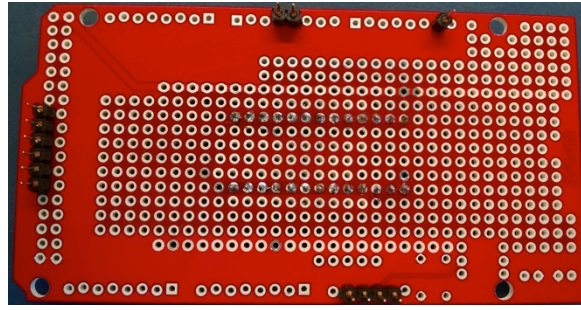
Step 1: Connect headers to MegaShield

Front:



Solder two rows of 13 pins onto the MegaShield to mount the two detectors. The acrylic housing is designed for the detectors to be mounted exactly as shown.

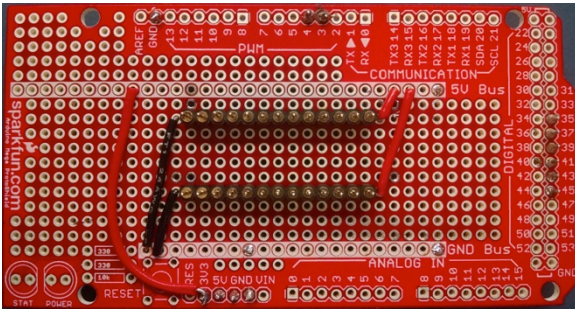
Back:



Solder pins into the power and ground. Do not solder pins into the pair of ground pins shown at the bottom right of this image or the hexagonal standoffs will not fit. Additional pins may be added for stability.

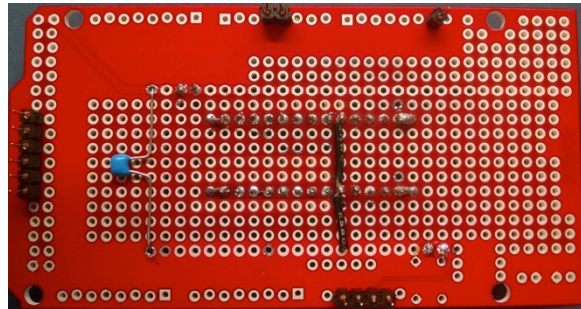
Step 2: Connect the power and ground

Front:



Solder the power to the V_{DD} pins and the ground to the V_{PP} pins of the detector as shown. Connect the 3.3V pin to the power bus.

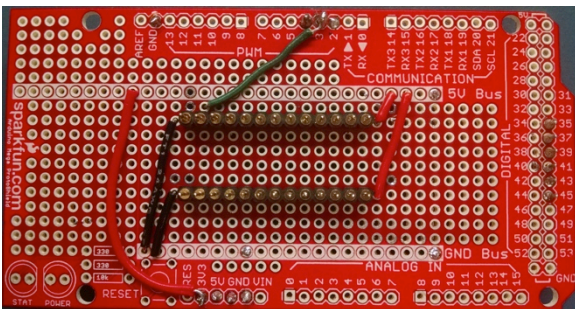
Back:



Solder the ground to the GND pins of the two detectors. Solder the 0.1 μF bypass capacitor between the power and ground.

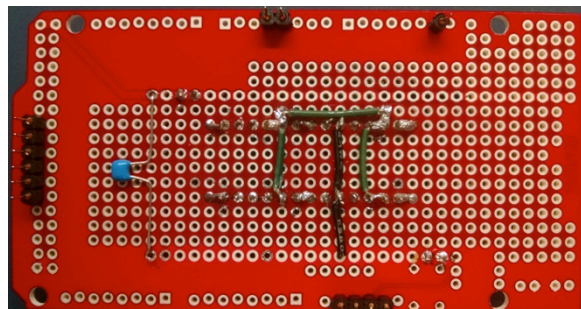
Step 3: Connect the serial input and hold

Front:



Solder a connector from Arduino PWM pin 3 to the SI1 pin of detector 1.

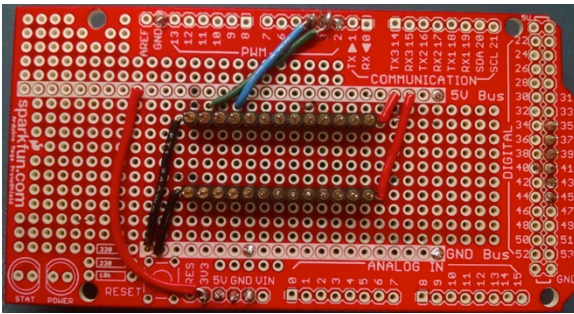
Back:



Solder connectors from SI1 of detector 1 to SI1 of detector 2. Solder a connector from the SI1 to SI2. Solder a connector from SI2 of detector 1 to SI2 of detector 2. Solder SI pins to neighboring HOLD pins

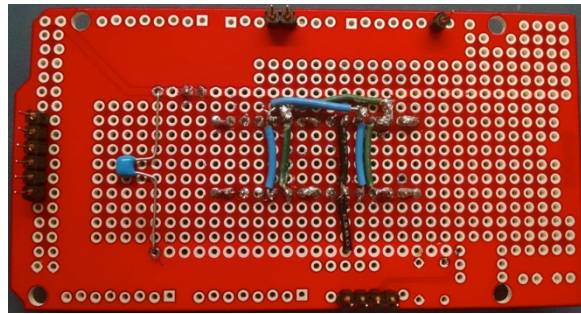
Step 4: Connect the clock

Front:



Solder a connector from Arduino PWM pin 4 to the CLK1 pin of detector 1.

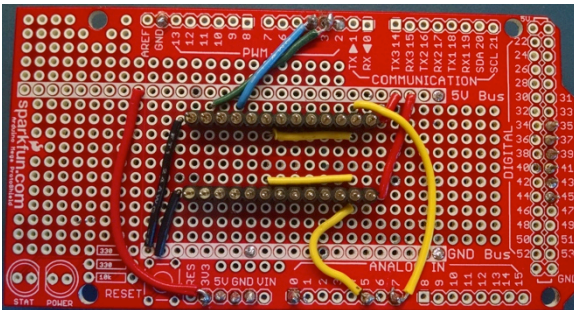
Back:



Solder connectors from CLK1 of detector 1 to CLK1 of detector 2. Solder a connector from the CLK1 to CLK2. Solder a connector from CLK2 of detector 1 to CLK2 of detector 2.

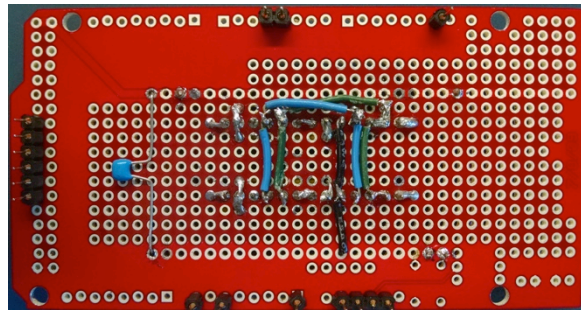
Step 5: Connect the analog outputs

Front:



Solder a connector from AO1 to AO2 for each detector. Solder a connector from detector 1 AO2 to Arduino Analog In pin 7. Solder a connector from detector 2 AO2 to Arduino Analog In pin 5.

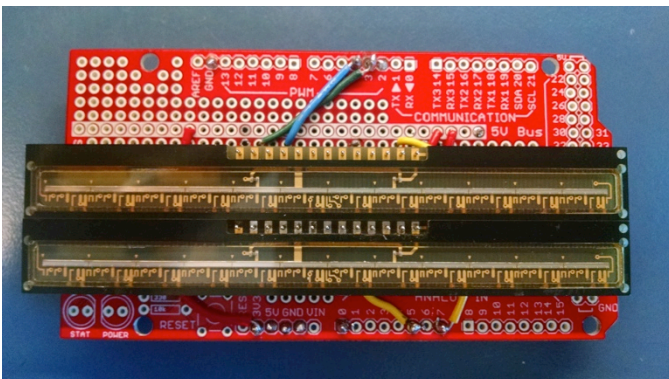
Back:



Solder analog output wires to detector pins.

Step 6: Attach detectors and arduino board

Front:



Connect detectors to pin headers. Soldering not required as heat may damage detectors. Plug in shield with detectors to Arduino Due board.

Step 7: Load firmware code

Connect Arduino to computer using the microUSB programming port.

Download firmware code, open in Arduino software, and upload sketch to device.

Firmware for detectors in serial

(https://github.com/kcarbonye/SAIM_calibration/tree/master/SAIM_arduino_serial)

Firmware for detectors in parallel

(https://github.com/kcarbonye/SAIM_calibration/tree/master/SAIM_arduino_parallel)

Step 8: Laser cut acrylic housing

96-well plate sized Arduino case (https://valelab.ucsf.edu/~kcarbonye/20151202_calibrator.ai)

Perspex front plate (https://valelab.ucsf.edu/~kcarbonye/20151204_calibrator_front.ai)

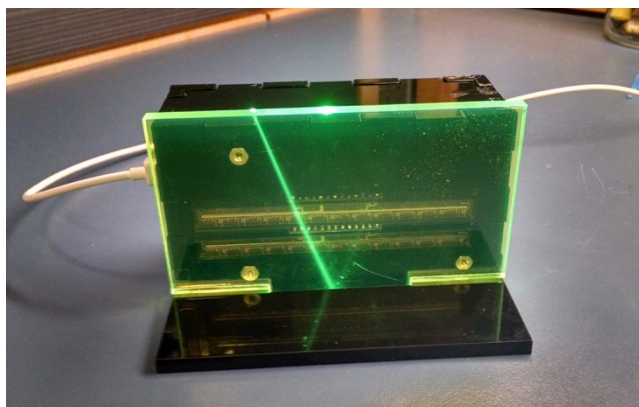
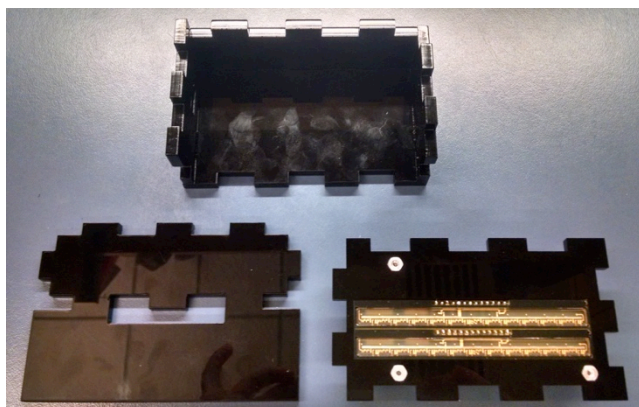
These files are intended for use with 0.25" cast acrylic. For the acrylic front plate, we recommend:

405 nm laser: Red fluorescent acrylic from Tap Plastics

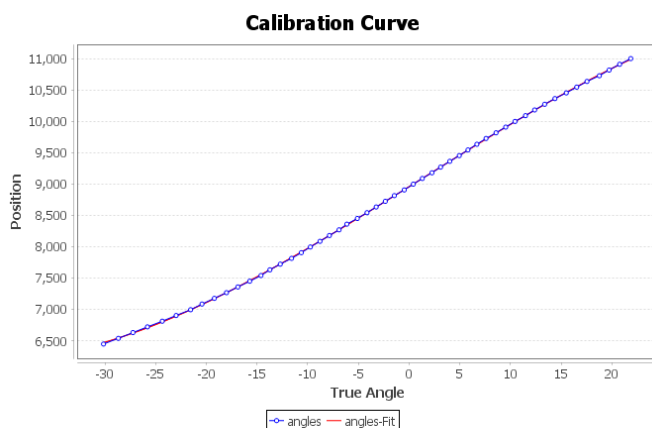
488 nm laser: Blue or green fluorescent acrylic from Delvies

561 nm laser: Blue fluorescent acrylic from Delvies

Step 9: Assemble device



Step 10: Run laser angle calibration using μ Manager plugin



μ Manager plugin development hosted at:

https://github.com/kcarbonye/SAIM_calibration

Example calibration curve used for SAIM data acquisition plotted as motor position (A.U., y-axis) versus refractive index corrected angle (degrees, x-axis)